Neurotoxicology 104 (2024) 45–55

Contents lists available at ScienceDirect

Neurotoxicology

journal homepage: www.elsevier.com/locate/neuro

Do toenail manganese and iron levels reflect brain metal levels or brain metabolism in welders?

Gianna Nossa [a], Humberto Monsivais [a], Chang Geun Lee [a], Grace Francis [a], Ellen M. Wells [a,b], Jae Hong Park [a], Ulrike Dydak [a,c,*]

[a] School of Health Sciences, Purdue University, West Lafayette, IN, United States
[b] Department of Public Health, Purdue University, West Lafayette, IN, United States
[c] Department of Radiology and Imaging Sciences, Indiana University School of Medicine, Indianapolis, IN, United States

ARTICLE INFO

Keywords:
Manganese
Toenails
MRI
Biomarkers
Welding

ABSTRACT

Inhalation of welding fumes can cause metal accumulation in the brain, leading to Parkinsonian-like symptoms. Metal accumulation and altered neurochemical profiles have been observed using magnetic resonance imaging (MRI) in highly exposed welders, being associated with decreased motor function and cognition. While MRI is impractical to use as a health risk assessment tool in occupational settings, toenail metal levels are easier to assess and have been demonstrated to reflect an exposure window of 7–12 months in the past. Yet, it is unclear whether toenail metal levels are associated with brain metal levels or changes in metabolism, which are the root of potential health concerns. This study investigates whether toenail manganese (Mn) and iron (Fe) levels, assessed at several time points, correlate with brain Mn and Fe levels, measured by MRI, as well as brain GABA, glutamate (Glu), and glutathione (GSH) levels, measured by Magnetic Resonance Spectroscopy (MRS), in seventeen Mn-exposed welders. Quantitative T1 and R2* MRI maps of the whole brain, along with GABA, Glu, and GSH MRS measurements from the thalamus and cerebellum were acquired at baseline (T0). Toenail clippings were collected at T0 and every three months after the MRI for a year to account for different exposure periods being reflected by toenail clippings and MRI. Spearman correlations of toenail metal levels were run against brain metal and metabolite levels, but no significant associations were found for Mn at any timepoint. Cerebellar GSH positively correlated with toenail Fe clipped twelve months after the MRI ($p = 0.05$), suggesting an association with Fe exposure at the time of the MRI. Neither thalamic GABA nor Glu correlated with toenail Fe levels. In conclusion, this study cannot support toenail Mn as a proxy for brain Mn levels or metabolic changes, while toenail Fe appears linked to brain metabolic alterations, underscoring the importance of considering other metals, including Fe, in studying Mn neurotoxicity.

1. Introduction

Excess exposure to manganese (Mn) can have a toxic effect on the brain. In occupational settings, the continuous inhalation of welding and smelting fumes may lead to Parkinsonian-like symptoms, including deteriorated cognitive, psychiatric, and motor function. (Cowan et al., 2009; Josephs et al., 2005; Lucchini et al., 2012) Overexposure has been associated with interrupting dopaminergic transmission in the striatum, (Guilarte et al., 2008) increasing oxidative stress in mitochondria within the basal ganglia, (Tuschl et al., 2013) and causing irregular glutamatergic and γ-aminobutyric acid (GABA)-ergic signaling, (Dydak et al., 2011) the primary pathways for excitatory and inhibitory circuitry in the basal ganglia.

Due to its paramagnetic properties, Mn deposition in the brain shortens the longitudinal relaxation time T1, which allows for a non-invasive measurement of brain Mn using magnetic resonance imaging (MRI). Studies have reported the longitudinal relaxation rate R1 ($R1 = 1/T1$) to be linearly proportional to Mn deposition in animal models with high exposure. (Dorman et al., 2006; Duck Park et al., 2007; Fitsanakis et al., 2006) In humans, R1 values have been found to be increased in occupational welders overexposed to Mn. (Criswell et al., 2012, 2015; Dydak et al., 2011; Long et al., 2014a; Monsivais et al., 2024) In addition to Mn, welding fumes also contain a high percentage of iron (Fe). Fe deposition in the brain can also be measured using MRI

* Correspondence to: School of Health Sciences, Purdue University, 550 Stadium Mall Drive, West Lafayette, IN 47906, Unites States.
E-mail address: udydak@purdue.edu (U. Dydak).

https://doi.org/10.1016/j.neuro.2024.07.007
Received 5 April 2024; Received in revised form 14 June 2024; Accepted 10 July 2024
Available online 11 July 2024

as its paramagnetic properties enhance the effective relaxation rate R2* and it is commonly used as a biomarker of Fe accumulation in the brain. (Haacke et al., 2005) It has been used as a tool to evaluate Fe accumulation related to Parkinson's and Alzheimer's Diseases. (Du et al., 2011; Gelman et al., 1999; Péran et al., 2010; Rossi et al., 2014; Ulla et al., 2013) However, the role of Fe in Mn-induced neurotoxicity is still unclear. Since Fe is a major component of welding fumes and can be measured both in toenail tissue and by MRI, it is worthwhile to also explore whether Fe toenail levels are associated with brain Fe levels or changes in brain metabolism due to welding fume exposure.

MRI offers another noninvasive avenue to assess the effects of Mn neurotoxicity via the changes in the brain's neurochemical composition through proton magnetic resonance spectroscopy (^{1}H-MRS). Our group has demonstrated elevated thalamic GABA levels, measured by edited ^{1}H-MRS, in response to high exposure to Mn in welding fumes, (Dydak et al., 2011; Ma et al., 2018) which was found to be reversible if exposure is decreased. (Edmondson et al., 2019) Furthermore, other human studies have shown that neurochemical changes are associated with decreased cognitive and motor function. (Chang et al., 2009; Kim et al., 2007; Long et al., 2014b) While MRI offers a window into brain structural and chemical changes, it is not a practical tool for risk assessment in the individual worker due to the high cost associated with it.

Possible biomarkers of exposure to metals include blood, plasma, serum, urine, bone, hair, saliva, and nails. (Karyakina et al., 2022) In particular, toenail metal levels have been explored by multiple groups as a practical biomarker of exposure to welding fumes. (Grashow et al., 2014; Laohaudomchok et al., 2011.; Ward et al., 2018) Toenail Mn levels have been shown by our group, (Ward et al., 2018) and others, (Grashow et al., 2014; Laohaudomchok et al., 2011) to correlate best with exposure levels between 7 and 12 months prior to clipping. Because toenail Mn levels were demonstrated to have the capacity to categorize individuals into exposure groups (Ward et al., 2018), and since both toenail levels and Mn-induced hyperintensities in brain MRIs are indicators of Mn uptake and deposition in the body, we hypothesize that these measurements maybe associated with each other. However, no such correlation was found in past studies where brain Mn (quantified by changes in MRI) and Mn in the toenail clippings were measured on the same day. (Edmondson et al., 2019) One of the challenges lies in identifying the correct time window for toenail clippings in relation to MRI scans. Mn clears the brain with a half-life of approximately 3 months in case of cessation of exposure (Grünecker et al., 2013; O'Neal and Zheng, 2015) and the longitudinal relaxation rate R1 in brain MRIs has been reported to capture changes in Mn exposure over the past 3 months in individual workers. (Edmondson et al., 2019; Lewis, Flynn, et al., 2016) Given that it takes approximately nine months for internalized Mn to reach the tip of a toenail, measurements of brain Mn and toenail Mn provide information on different time windows of exposure, which was seen by the fact that MRI values did not correlate with toenail levels if there was any change in exposure over the past year. (Yeh et al., 2015) A longitudinal sampling of toenails, especially over the year after the MRI scan, is necessary to better understand the relation between these two markers of internalized Mn burden.

Changes in neurotransmitter pathways and neurochemical concentration changes in the brain, caused by Mn neurotoxicity, are at the basis of potential adverse health effects and diminished cognitive and motor function. (Chang et al., 2009; Kim et al., 2007; Long et al., 2014b) Thalamic GABA levels have been found to change according to variations in exposure within two years.(Edmondson et al., 2019) Thus, if a marker of individual metal exposure should also serve as a marker of individual health risk, that marker should relate to imaging biomarkers of the brain's Mn and Fe content and/or the brain's metabolic reaction to the metal burden. Therefore, this study investigates whether toenail Mn and Fe levels are indicative of brain Mn and Fe levels and changes in brain GABA, Glu, and glutathione (GSH – primary antioxidant in the brain) levels in two brain regions of Mn-exposed welders. In this longitudinal observational study, a group of continuously Mn-exposed welders was examined using MRI/^{1}H-MRS, and their toenails were subsequently collected at 4 intervals over the following year.

2. Methods

2.1. Subject recruitment

A subgroup of 22 full-time welders (21 male, 1 female) employed at a truck trailer manufacturer was recruited for this longitudinal study on toenail clippings, which was nested into a larger neuroimaging study of occupationally exposed welders (parent study). Welders were mostly using metal inert gas (MIG) welding and worked 8–10 h shifts for 5–6 days per week. Inclusion criteria consisted of being aged 18 years or older, being safe to obtain an MRI scan, and being employed as a welder by the trailer manufacturer for at least the past year. Welders continued in their jobs and were exposed to welding fumes throughout this study. Additionally, six non-exposed controls were recruited from the university environment to provide annual toenail clippings as part of the parent study. None of the subjects had a history of neurological or psychiatric disorders. This study was approved by the Institutional Review Board at Purdue University. Written informed consent was obtained from all subjects prior to participation in the study.

As part of the parent study, all welders visited the Purdue MRI facility, where they were interviewed about their medical history, life habits (e.g., diet, smoking, drinking), and about their work history. Further, they completed a series of motor and cognitive tests, received an MRI/^{1}H-MRS scan of approximately one hour and provided toenail clippings. Personal air sampling was conducted on each subject during a full 8-hour shift at their workplace following their visit to the MRI facility, as described in Ward at al. 2018. Specifically for this study, starting at the time of the initial MRI visit (T0), additional toenail clippings were collected every three months for a year, denoted as T3, T6, T9, and T12, as illustrated in Fig. 1. Since this is an observational study, welders continued to work full-time throughout the duration of the study (T0-T12) and during the full year before the MRI with varying exposures. Toenail clippings from the six control subjects were only obtained at T0 and T12 to compare variation over time.

2.2. Toenail processing

Toenail clippings were collected and carefully preserved in envelopes, each labeled with subject identification until the preparation phase. In the preparation process, visible dirt and impurities on the toenail surfaces were removed manually. Subsequently, the clippings were placed in 10 mL test tubes. To remove external contaminants, the toenail samples were cleaned using a non-ionic surfactant (Triton X-100, 1 % in deionized water) in an ultra-sonication bath for 1 hour. The clippings were then rinsed three times with deionized water (ASTM II) and dried in an oven for more than 24 hours. The dried clippings were then weighed using a microscale. The toenail samples were digested in 5 mL of 70 % nitric acid (HNO_3; ARISTAR® ULTRA, Ultrapure for trace metal analysis, VWR International, U.S.A.) using a microwave digestion system (MARS 6, CEM co., U.S.A.) for 15 minutes at 200°C. The prepared samples in test tubes were diluted to a 2 % nitric acid concentration and subsequently delivered to the campus-wide Inductively Coupled Plasma-Optical Emission Spectrometer (ICP-OES) facility for metal analysis. (Lee et al., 2023) Three ICP-OES measurements were taken of each participant's toenail sample dilutions and results were averaged. The metal concentrations in toenail samples were calculated by dividing the ICP-OES average results by the weight of the toenail clippings.

2.3. MRI acquisition

MRI and ^{1}H-MRS exams were performed using a 3 T Siemens Prisma MRI scanner equipped with a 20-channel head coil. The imaging

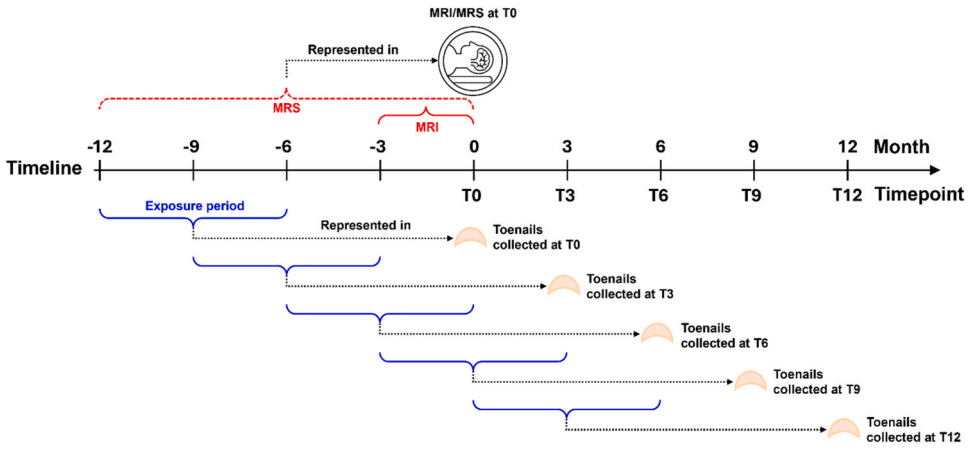

Fig. 1. Study timeline: MRI and initial toenail collection occurred at T0. Additional toenail collections occurred 3, 6, 9, and 12 months after MRI (T0, T3, T6, T9, and T12). The blue brackets show the exposure periods that are best represented by the respective toenail samples according to the literature. The exposure period best reflected by the MRI is assumed to be the three months prior to the MRI, shown in red. The exposure period reflected by metabolic changes is unknown, but likely longer than three months, shown in a red dashed bracket. This study design should enable the MRI and toenail clippings of at least one of the timepoints to be representative of an overlapping exposure period.

protocol consisted of a fast T2-weighted sequence, acquiring coronal, sagittal, and axial images (TR/TE = 1500/81 ms, resolution: 0.8 ×0.8 ×4 mm^3) for placement of the MRS volumes of interest (VOIs) followed by a high-resolution T1-weighted MPRAGE sequence (TR/TE = 2000/2.05 ms, resolution: 1 × 1 × 1 mm^3). Quantitative T1 mapping was achieved using a 3D variable flip angle (VFA) spoiled gradient recalled echo technique (TR/TE = 10/2 ms, resolution: 1 × 1 × 1 mm^3, a = 3° and 17°). A transmit field (B_1^+) map was also acquired to correct for radiofrequency field inhomogeneity. Lastly, quantitative R2* maps were acquired using a 3D multi-gradient recalled echo sequence (mGRE) (TR/dTE/TEs = 48/4.06/6.28–42.82 ms, resolution: 0.8 × 0.8 × 3.0 mm^3).

2.4. R1 and R2* region of interest (ROI) analysis

Anatomical T1-weighted images, T1 and R2* maps were exported as DICOM files from the scanner and converted to NIfTI files using SPM12. Individual T1 and R2* maps were co-registered to the T1w images using affine transformations with the normalized mutual information cost function in SPM12. Next, the T1w images were automatically aligned to the Montreal Neurological Institute (MNI-152) T1-weighted template using the *Auto-reorient* feature of the hMRI Toolbox, (Tabelow et al., 2019) which also allows us to apply the same spatial transformations to the T1 and R2* maps. This step ensures that all images are in the same general orientation prior to processing and reduces the number of errors encountered during processing. The T1-weighted images were then segmented into grey matter (GM), white matter (WM) and cerebrospinal fluid (CSF) using tissue probability maps (TPMs) specifically derived from multi-parametric maps. (Lorio et al., 2014) GM and WM images were non-linearly transformed to standard MNI space, without modulation, using the DARTEL tool (Ashburner, 2007) and the transformation matrices were applied to corresponding T1 and R2* maps. At this point, all three sets of images (T1-weighted, T1, and R2* maps) were aligned in the MNI common space.

R1 (R1 = 1/T1) and R2* relaxation rates were measured bilaterally in regions of interest (ROIs) placed in the globus pallidus (GP), putamen (Put), substantia nigra (SN), frontal white matter (FWM), and the dentate nucleus (DN) in the cerebellum. FSLeyes (McCarthy, 2023) was used to generate the ROI masks and MRIcron (Rorden and Brett, 2000) to extract the relaxation values. R1 (a proxy for Mn) and R2* (a proxy for Fe) values from the left and right hemispheres were averaged for every brain structure. The placement of the defined ROIs is illustrated in Fig. 2.

2.5. MRS acquisition and analysis

GABA+, Glx, and GSH measurements were acquired using the HERMES sequence (Chan et al., 2016) (TR/TE = 2000/80 ms) with the editing pulses centered on 1.9 ppm (edit ON for GABA), 4.7 ppm (edit ON for GSH), and 7.5 ppm (edit OFF for both). 256 averages were

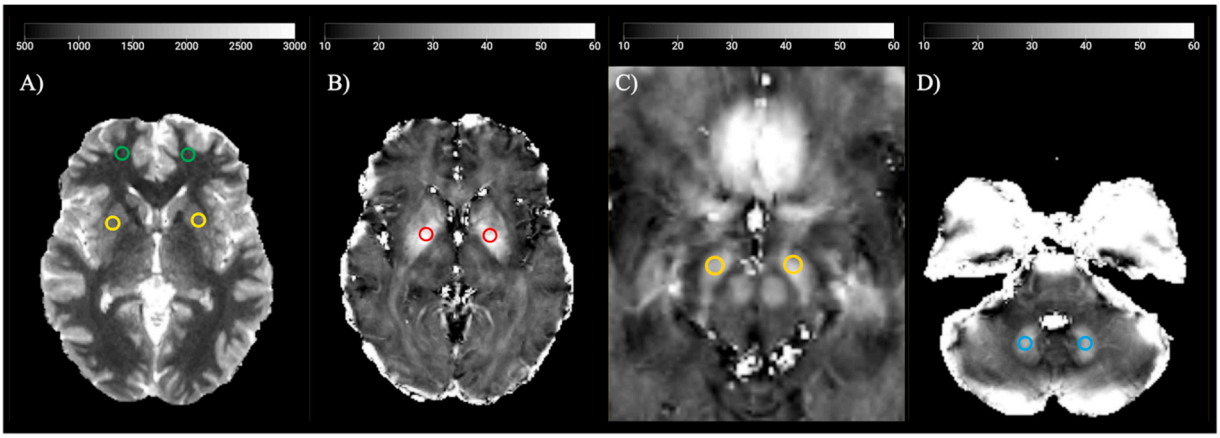

Fig. 2. Axial slices of T1 map (A) and R2* map (B, C, and D) showing ROIs for the FWM (green), Put (yellow), GP (red), SN (orange), and DN (light blue). Abbreviations: FWM, frontal white matter; Put, putamen; GP, globus pallidus; SN, substantia nigra; DN, dentate nucleus.

acquired for edit ON and edit OFF spectra in an interleaved fashion. 8 averages of water reference scans without water suppression were acquired for frequency and phase correction. To determine the thalamic and cerebellar metabolite levels, the MRS VOI was centered on the right thalamic region and right cerebellar lobe (30 mm × 30 mm × 25 mm), as shown in Fig. 3. Spectra were analyzed using Gannet (Version 3.3). (Edden et al., 2014) Cerebrospinal fluid (CSF) correction was performed within the Gannet toolbox using *GannetSegment*, and the CSF-corrected metabolite values were used for further statistical analysis.

2.6. Statistical analysis

Out of the 22 welders who were recruited, one was excluded due to bad quality MRI/^{1}H-MRS data, and one did not provide any toenail clippings. Three more welders were excluded due to their toenail clippings being deemed unreliable because of the calibration error of the ICP-OES equipment. Overall, 17 welders consisting of 16 males and 1 female has a complete MRI/^{1}H-MRS and toenail clipping analysis for time point zero (T0) and were included in the statistical analysis. Due to attrition over time, subsequent time points had fewer and varying sample sizes for the toenail metal concentrations, as indicated in Table 2.

For correlation analysis, two hypotheses were tested: a) toenail metal levels at time points T6-T12 are correlated to brain metal levels as measured by R1 and R2* at T0; b) toenail metal levels at time points T6-T12 are associated with neurochemical concentration levels in the thalamus and the cerebellum measured at T0. All statistical analyses were performed within the R environment (Posit team (2023), version 2023.6.0.421). A Shapiro-Wilk test of normality was performed on all variables prior to analysis. Toenail Mn levels, R1 and R2* values were normally distributed, while toenail Fe levels and several MRS values were found to be nonnormally distributed. Based on these results, with the small number of subjects and high potential for outliers to affect the results, linear relationships were assessed through nonparametric means using Spearman rank correlations. Multiple comparison testing was applied using the Benjamini & Hochberg method ("FDR") at $\alpha = 0.05$. Unadjusted and adjusted p-values are presented when applicable.

Due to the repeated measures of toenail metal levels, we performed an additional analysis using the generalized estimating equation (GEE) model, which accounts for the correlation within repeated measurements for a welder over time and provides estimates of the average response across all subjects. (K.-Y. Liang and Zeger, 1986) The models were constructed to assess the same relationships as described above using the *gee* package in R. The models were constructed to assess the same relationships as described above using the *gee* package in R. Although Generalized Mixed Models (GLMM) were also considered, we encountered significant convergence issues, likely due to the small sample size. Consequently, GEE was chosen as a more practical alternative given that it can handle the correlation structure of our data and our small sample size.

Inter- and intrasubject coefficients of variation (CV%) are reported to compare the variation of toenail metal levels between welders and controls. The average intersubject CV% was calculated by averaging the intersubject CVs for timepoints T0 and T12, whereas the intrasubject CV % was calculated by averaging the intrasubject CV for timepoints T0 and T12 over all subjects within each group. Lastly, we calculated the intrasubject correlations (ICCs) estimates and their 95 % confidence intervals of the toenail metal levels over time using the *ICC* function from the *psych* package in R, based on a single rater/measurement, consistency, two-way mixed-effects model (ICC(3)). ICC(3) offers insight into the consistency of individual time point measurements (Koo and Li, 2016).

3. Results

A summary of the participants' demographics and toenail Mn and Fe concentrations at T0 is reported in Table 1.

The mean air Mn concentration inhaled by the welders was measured as 137.0 μg/m^3 (range: 0.5 – 562.3 μg/m^3) and 1114.2 μg/m^3 (range:

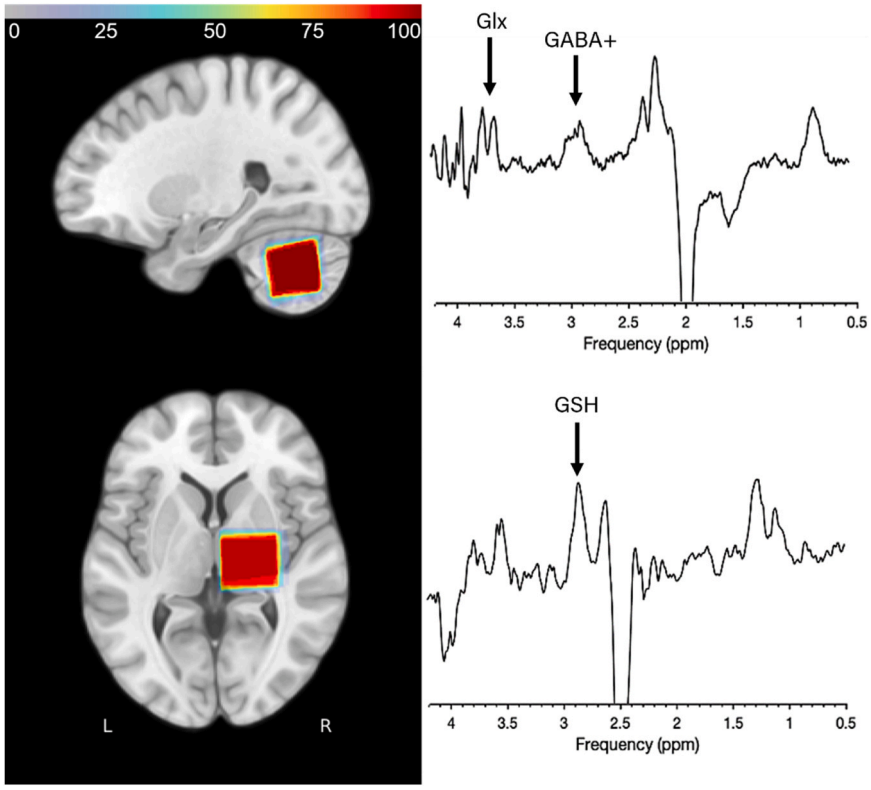

Fig. 3. The consistency map of *v*oxel placements superimposed on the MNI152 template, demonstrates high reproducibility for the cerebellum (top) and thalamus (bottom); representative GABA and GSH spectra.

Table 1
Demographics of study participants.

Subject Characteristics	Welders (n = 17)
Age (years) [mean ± SD]	45.6 ± 12.5
Sex	16 M, 1 F
Welding experience	2
≤1 yr	6
2–10 yrs	1
11–20 yrs	7
21–30 yrs	1
31+ yrs	
Race/Ethnicity	
Black or African American	2
White	12
Hispanic/Latino	3
Toenail metal levels (μg/g)*	
Manganese (Mn)	
Min:	-0.2
1st Quartile:	5.2
Median:	7.1
Mean:	7.1
3rd Quartile:	9.0
Max:	17
Iron (Fe)	
Min:	11.6
1st Quartile:	25.1
Median:	43.8
Mean:	50.1
3rd Quartile:	67.2
Max:	138.8

* Summary statistics for toenails collected from the 17 welders including those without a complete set of toenail clippings for every time point.

3.7 – 5264.9 μg/m^3) for Fe, measured by personal air sampling, as described by Ward et al., (2018). Metal level analysis of all toenail samples from all time points was performed in the same batch of ICP-OES analysis to avoid fluctuations due to batch differences. Toenail Mn levels in this cohort of welders were above 3.0 μg/g for all time-points (*Supplemental Figure 1*) with a mean of 7.5 ± 2.3 μg/g for the first time point, T0.), whereas the mean toenail Mn values for the control group at T0 was about half (3.3 ± 1.9 μg/g). Mean toenail Fe levels in the welders and controls at T0 were 40.0 ± 22.0 and 19.5 ± 15.8 μg/g, respectively. Since the toenail Fe values were not normally distributed, the median and interquartile (IQR) values of toenail Mn and Fe concentrations for welders and controls are presented in Table 2, as are averaged inter- and intrasubject CVs.

Table 2
Toenail Mn and Fe concentrations for each timepoint.

	Welders		Controls	
Timepoint	**Mn (μg/g)** Median (IQR)	**Fe (μg/g)** Median (IQR)	**Mn (μg/g)** Median (IQR)	**Fe (μg/g)** Median (IQR)
T0	7.8 (4.6) n = 17	29.9 (51.0)	3.3 (1.5) n = 6	19.5 (11.1)
T3	7.1 (4.7) n = 10	41.5 (49.7)		
T6	7.4 (1.9) n = 9	44.1 (15.7)		
T9	5.8 (2.9) n = 8	46.6 (37.7)		
T12	5.9 (2.2) n = 8	52.6 (35.8)	2.8 (2.1) n = 6	22.3 (18.9)
Avg. Inter-CV:†	39 %	62 %	54 %	69 %
Avg. Intra-CV:†	28 %	33 %	23 %	34 %

†Inter- and intra- subject CV% for Mn and Fe are calculated using toenails collected at T0 and T12, and averaged across timepoints, or across subjects, respectively.

3.1. Correlation between toenail metal levels and MRI metal levels

A summary of ROI values, serving as proxies for Mn and Fe levels in respective brain regions, is presented in Table 3. We found no statistically significant correlations between Mn toenail levels and R1 values in any of the brain ROIs. As for Fe, we found a statistically significant positive correlation between Fe toenail levels at T3 and R2* in the DN (r = 0.76, p = 0.04); however, this loses significance when correcting for multiple comparisons using a false discovery rate (FDR) at 5 % (adj. p = 0.26). No other correlations were found between Fe toenail levels and R2* values. There were a couple of significant correlations within R1 values across brain regions. R1 in the GP was significantly correlated with R1 values in the Put (r = 0.46, p = 0.04, adj. p = 0.12) and the DN (r = 0.65, p < 0.001, adj. p = 0.009). R1 in the DN was correlated with R1 in the SN, but the significance did not hold after correcting for multiple comparisons (r = 0.47, p = 0.03, adj. p = 0.12). Correlation results are summarized in Fig. 4.

Correlation between toenail metal levels and brain metabolite levels

A summary of metabolite statistics for the thalamus and cerebellum is presented in Table 4. In the thalamus, we found a negative correlation between Glx and toenail Mn at T0 (ρ = −0.62, p = 0.01, adj. p = 0.08). Toenail Fe was found to negatively correlate with thalamic GABA+ at T0 (ρ = −0.62, p = 0.01, adj. p = 0.11) and T3 (ρ = −0.68, p = 0.05, adj. p = 0.24), and with Glx at T12 (ρ = −0.82, p = 0.03, adj. p = 0.16). Thalamic GSH was not found to correlate with either toenail metal at any timepoint. In the cerebellum, no significant correlation was found between GABA+, Glx, and GSH and toenail Mn at any timepoint. While cerebellar GSH was found to be positively correlated with toenail Fe at both T6 (ρ = 0.79, p = 0.03, adj. p = 0.14) and T12 (ρ = 0.88, p = 0.007, adj. p = 0.05), neither GABA+ nor Glx correlated with toenail Fe levels in the cerebellum. Correlation results are summarized in Fig. 5.

Results from the GEE models showed similar trends with the only significant result being the positive correlation between cerebellar GSH and Fe toenail levels (see *Supplemental Table 1*). In the simpler model (Spearman correlations), we found that cerebellar GSH and Fe toenail at T12 were the only statistically significant correlation after correcting for multiple comparisons. As it can be seen in Figs. 4 and 5, there is high correlation between the toenail metal levels at different time points (especially T0 and T3 for both Mn and Fe). The ICC(3) for Mn levels confirms a high intercorrelation for individual measurements (ICC = 0.81 CI: 0.67, 0.91). For Fe levels, the ICC(3) showed a more moderate intercorrelation for individual measurements (ICC = 0.63, CI: 0.46, 0.81).

4. Discussion

To the best of our knowledge, this is the first *in vivo* longitudinal study in welders to investigate the association between toenail metal levels as biomarkers of exposure to welding fumes and MRI markers of brain Mn and Fe levels. This study is observational in a regular working environment in a factory, with no influence on changes in exposure over time. While a lot of effort was put into reminding study participants to provide their toenail clippings every three months, the smaller sample

Table 3
Summary of ROI statistics for R1 and R2* values.

	Globus Pallidus Mean ± SD	**Putamen** Mean ± SD	**Frontal White Matter** Mean ± SD	**Substantia Nigra** Mean ± SD	**Dentate Nucleus** Mean ± SD
R1 (1/s)	0.96 ± 0.10	0.78 ± 0.06	0.99 ± 0.13	0.88 ± 0.08	0.90 ± 0.05
R2* (1/s)	52.8 ± 17.6	52.1 ± 21.1	23.8 ± 5.5	40.3 ± 12.6	32.5 ± 9.4

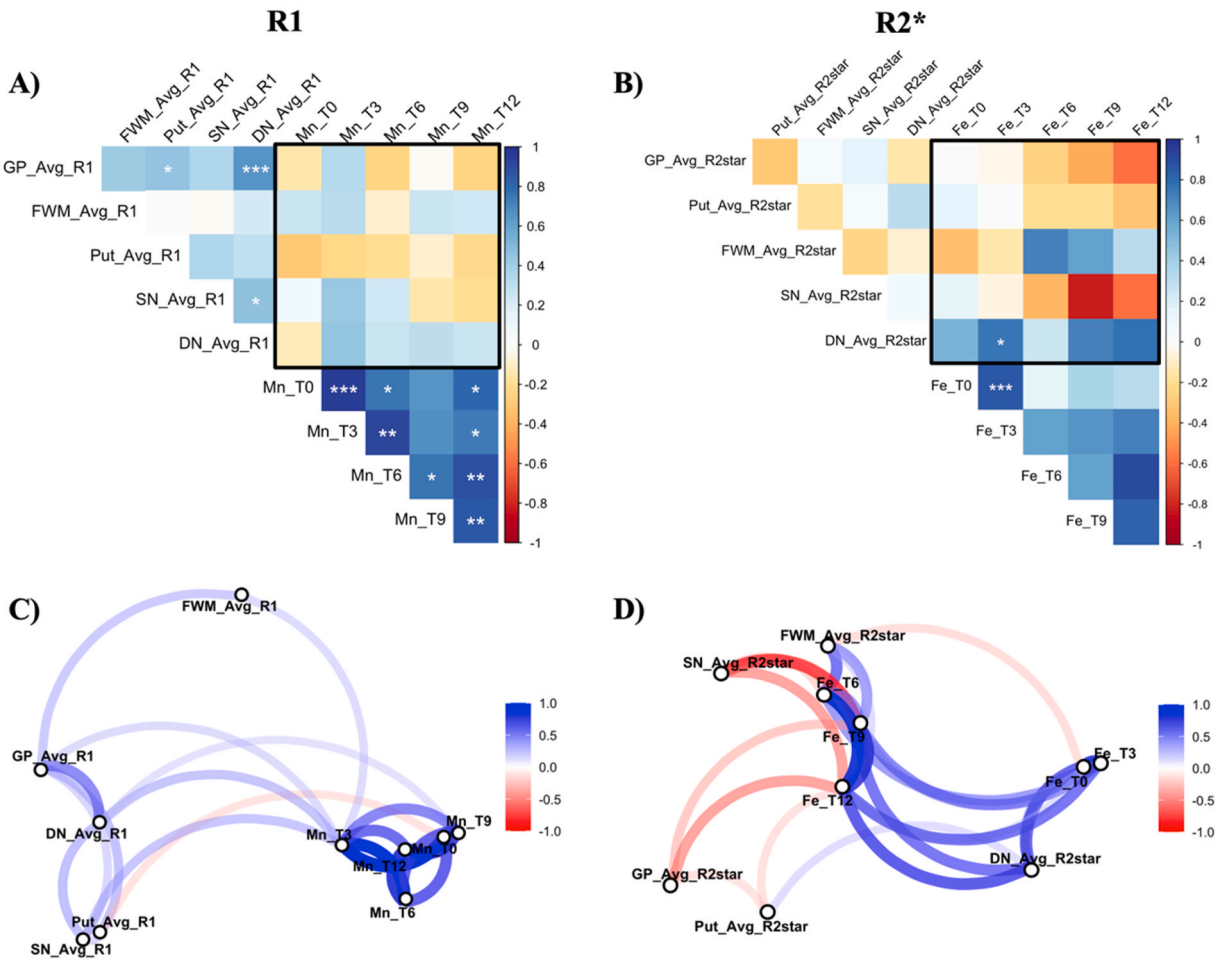

Fig. 4. Top: Correlation matrix of brain Mn levels (R1) and toenail Mn levels (A), and brain Fe levels (R2*) and Fe toenail levels (B). Darker blue indicates a strong positive correlation while darker red indicates a negative correlation. Statistical significance is indicated with asterisks as *p = 0.05, **p = 0.01, and *** p = 0.005 (uncorrected for multiple comparisons). T0 indicates the toenail metal levels at the time of the MRI scan, and T3–12 indicates toenail metal levels so many months post MRI scan. Only matrix elements within the black boxes indicate correlations between toenail metal levels and brain metal levels. Bottom: Correlation network of C) R1 values in the main regions of the basal ganglia, FWM, SN, and DN in the cerebellum with Mn toenail levels; and D) R2* values in the same brain regions with Fe toenail levels. Only the correlations with Spearman coefficients higher than 0.3 are shown. Red indicates negative correlations while blue indicates positive correlations. The strength of the correlation coefficients is indicated by the opacity of the paths. Abbreviations: GP, globus pallidus; FWM, frontal white matter; Put, putamen; SN, substantia nigra; DN, dentate nucleus.

Table 4
Summary of Metabolite statistics for the Thalamus and Cerebellum.

	[GABA+] i.u. Mean ± SD	**[Glx] i.u.** Mean ± SD	**[GSH] i.u.** Mean ± SD
Thalamus	3.51 ± 1.72	9.41 ± 2.72	1.24 ± 1.41
Cerebellum	3.41 ± 1.92	8.46 ± 2.52	1.19 ± 0.48

size of toenail clippings at time points after the MRI is a clear limitation that needs to be kept in mind throughout the discussion.

Upon inhalation, Mn is absorbed by the olfactory bulbs via the primary olfactory neurons and subsequently transported both within and between neurons to reach various regions of the brain. (Tjillve et al., 1996) In homeostasis, Mn enters cells through a variety of metal ion transporters such as the Divalent Metal Transporter1 (DMT1) and Transferrin Receptor (TfR), both of which have high affinity for Mn and Iron (Fe). (Chen et al., 2015; Horning et al., 2015; Tuschl et al., 2013) Toenails are composed of keratins, a type of fibrous protein that includes disulfide bridges, believed to bind to metals present in the body as they grow.(Raab and Feldmann, 2005; Slotnick and Nriagu, 2006)Metals excreted by the body can attach to nails due to their high sulfur content; however, it should be noted that the process by which metals are integrated into nail structures is still not completely understood.

We primarily examined brain areas of the basal ganglia, the globus pallidus and putamen, known to have an excess accumulation of Mn (Baker et al., 2015; Criswell et al., 2012, 2019; Dydak and Criswell, 2015; Lewis et al., 2016) in addition to the frontal lobe, as previous studies animal and human studies have shown that Mn also accumulates in the frontal white matter. (Dorman et al., 2006; Guilarte et al., 2006; Lee et al., 2015; Verina et al., 2013) We also explored the substantia nigra, which plays an important role in motor planning, reward-seeking, addiction, and other functions. (Nicola et al., 2000) Ma et al., (2018) showed that Mn deposition in the substantia nigra and globus pallidus was directly associated with exposure and elevated thalamic GABA. Excessive Mn can impair the function of the dopamine-producing neurons in the substantia nigra, although the exact mechanisms by which Mn affects these neurons are still under investigation. (Jankovic, 2005; M. Lin et al., 2020; Verhoeven et al., 2011) Furthermore, we included the dentate nucleus in the cerebellum as part of an exploratory analysis since it has been shown that increased R1 (a proxy for Mn) in the cerebellum is associated with the past three months of Mn exposure. (Monsivais et al., 2024) The cerebellum and its associated structures, including the dentate nucleus, are primarily responsible for coordination, balance, and fine-tuning of movements (Koziol et al., 2014) in

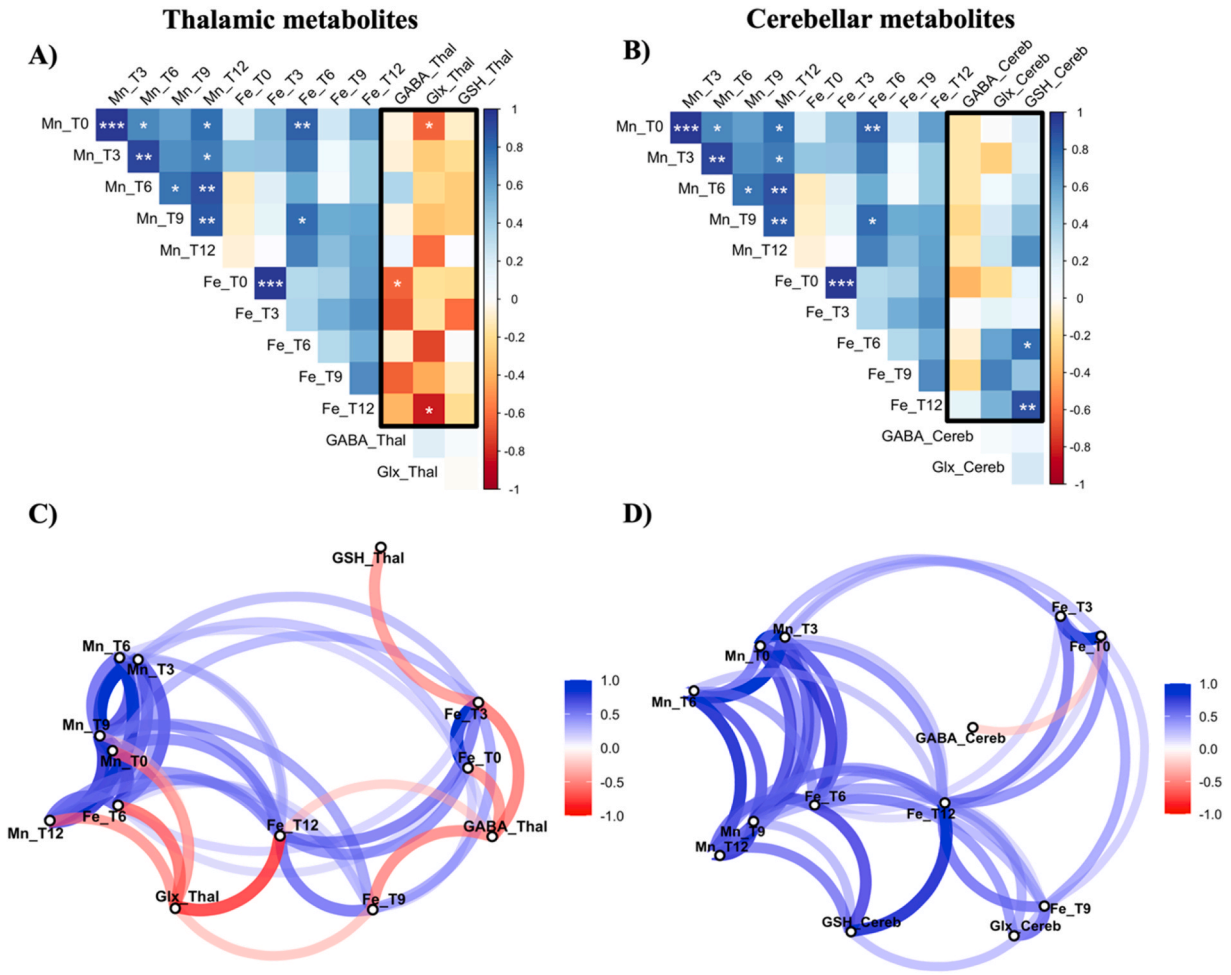

Fig. 5. Top: Correlation matrix of toenail metal levels and brain metabolites in the thalamus (A) and the cerebellum (B). Darker blue indicates a strong positive correlation while darker red indicates a negative correlation. Statistical significance is indicated with asterisks as *p = 0.05, **p = 0.01, and *** p = 0.005 (uncorrected for multiple comparisons). T0 indicates the toenail metal levels at the time of the MRI scan, and T3–12 indicates toenail metal levels so many months post MRI scan. Bottom: Correlation network of toenail Mn and Fe levels with C) thalamic GABA+, GSH, and Glx; and D) cerebellar GABA+, GSH, and Glx. Only the correlations with Spearman coefficients higher than 0.3 are shown. Red indicates negative correlations while blue indicates positive correlations. The strength of the correlation coefficient is indicated by the opacity of the paths.

addition to nonmotor cognitive, linguistic, and affective processes. (Baillieux et al., 2008; Beaton and Mariën, 2010; Murdoch, 2010; Schmahmann and Sherman, 1998; Stoodley and Schmahmann, 2010) While it is not yet clear how excess Mn in the cerebellum affects motor function, Mn-induced volume decrease has been reported to correlate with reduced performance in fine motor and executive function tasks in full-time welders. (Chang et al., 2013) In addition, Monsivais et al. showed association between lower performance in motor scores with increased Mn accumulation in the cerebellum. As for Fe, studies have found increased Fe concentrations in the substantia nigra, globus pallidus, and caudate of patients with Parkinson's Disease (Griffiths et al., 1999) and Alzheimer's Disease, (Lin et al., 2023) with increased Fe concentrations reported in the caudate, (Lee et al., 2016) and the frontal cortex, (Long et al., 2014a) however, the effect of excess Fe in the brain is not known.

Toenail metal levels in this cohort of welders were found to be similar to the values reported for the welder population of our former study, (Ward et al., 2018) which reported that toenail Mn discriminates between controls and welders with 91 % specificity and 94 % sensitivity at a toenail Mn concentration threshold of 4.14 μg/g. Toenail levels of all participating welders in this study were above that threshold, while the toenails from the control group were below this threshold. Ward et al. also reported average toenail Mn levels in welders to be 6.87 μg/g, which is in-line with our cohort's levels of 7.5 μg/g, and 3.3 μg/g in the control group. (Ward et al., 2018) This indicates that the welders were clearly exposed to Mn and Fe, which deposited in their toenails, and distinguished them from non-exposed subjects, as presented in *Supplemental Figure1*.

Nevertheless, in this cohort of U.S. welders, we found no statistically significant associations between brain Mn levels, measured by MRI, and toenail Mn levels collected quarterly over a year-long period. Based on animal studies, brain Mn shows up quickly upon exposure (Dorman et al., 2002; Grünecker et al., 2013) and is known to wash out with a half-life of approximately 3 months from the brain. (Takeda et al., 1995) In contrast, toenail metal concentrations measured in toenail clippings reflect exposure and deposition into the toenail tissue up to a whole year in the past, depending on the growth rate of toenails. Thus, our hypothesis was that brain metal levels as imaged by MRI and toenail metal levels might simply reflect different exposure windows. However, this study, while investigating specifically correlations between MRI and different time points of toenail clipping, was not able to shed light on any relationship. It is clearly possible that this is due to the limitation of the small sample size. Yet, the fact that both the inter- and intra-subject CVs for toenail Mn and Fe were comparable between welders and controls, suggests that, while toenail metal levels were elevated, their variation over the year was within a normal range. This may explain

why testing different timepoints of toenail clipping did not show another finding than the null-findings at T0, which already was reported previously in a different group of welders. (Edmondson et al., 2019) Edmondson et al. suggests that the lack of a correlation in his data was likely due to the different time windows of exposure reflected by toenails and MRI. Yet, he also found that lifelong cumulative exposure levels modulate the relation between change in exposure and change in R1, whereas no such modulation was found for the relationship between changes in toenail Mn with changes in past-year exposure. He already interpreted this to suggest that the process by which Mn accumulates in toenails is different than how it accumulated in brain or affects R1. Our results also may suggest that the relationship between metal deposits in the brain and in toenail tissue may be more complex than a simple timing issue, likely because metal accumulation in toenails occurs by a different mechanism than uptake of Mn and Fe into the brain, which can even be different for different brain regions.(Dorman et al., 2002) Furthermore, the physics of how Mn, Fe, and their mixture impact R1 and R2* in MRI adds another layer of complexity that might obscure a relationship of these internal metal depositions. (Zhang et al., 2009)

Indeed, our network plot visualization (Fig. 4*C*) of the correlations among selected brain regions involved in excess Mn accumulation and Mn toenail levels demonstrate that brain Mn levels and toenail Mn levels are far apart (weaker correlations). This may suggest that the pharmacokinetics of Mn distribution in the human body are too complex to allow for a simple relationship between brain and toenail Mn accumulation.

In the case of Fe, we see from our network plot that the relationship between brain Fe levels and toenail Fe levels is closer together (stronger correlations). Still none of these relationships survived correction for multiple comparisons, which may be due to the small sample size, or may indicate that the relationship between brain Fe levels and toenail Fe levels again is more complex than reflecting different exposure time frames.

In the central nervous system, Mn serves as a cofactor for numerous enzymic processes and is required for immune function and defense against reactive oxygen species (ROS). (Aschner and Aschner, 2005; Horning et al., 2015) While the mechanisms of Mn neurotoxicity are still not well understood, there have been many proposed etiologies, including the accumulation of Mn in the mitochondria, interfering with oxidative phosphorylation and leading to the production of ROS; and interaction with glutamine synthetase, interrupting the production of excitatory and inhibitory neurotransmitters, Glu and GABA+, respectively. (Horning et al., 2015; Tuschl et al., 2013)

We therefore also explored the associations between changes in the brain's neurochemical composition, as assessed by MRS, regarding the cerebellum and thalamus. The ganglia-thalamo-cortical pathway primarily plays a role in both voluntary movements and the emotional, motivational, and cognitive processes that underlie and guide these movements. (Haber and Calzavara, 2009) Previously, studies have found increased thalamic GABA+ levels in smelters with high Mn exposure, (Dydak et al., 2011) which was confirmed to relate to fine motor function. (Long et al., 2014b) While metabolite concentrations have been found to vary between brain regions, one group reported metabolite concentrations in the thalamus of a healthy control group to be approximately 2.51 i.u. for GABA+, 7.72 i.u. for Glx, and 1.22 i.u. for GSH. (Liang et al., 2024) We have estimated higher GABA+ (3.51 i.u.) and higher Glx (9.41 i.u.), which supports our previous findings of increased GABA in the thalamus of welders, (Ma et al., 2018). However, our estimation of GSH is comparable to the value Liang et al. reported for the healthy control group. In addition, animal studies of Mn exposure have found changes in GABA+ levels in other brain regions, including the cerebellum. (Lipe et al., 1999)

However, we found no statistically significant association between *thalamic* metabolites and either Mn or Fe in toenails. From our network plot visualization (Fig. 5*C*) of the correlations among thalamic GABA+, GSH, and Glx and Mn toenail levels we can see that brain metabolite levels and toenail Mn levels are far apart, indicating weaker correlations. This could also suggest that toenail Mn levels are not reflective of changes in metabolite levels at any time interval. When we consider toenail Fe, we see from our network plot stronger correlations between brain metabolite levels and toenail Fe deposition, especially between toenails collected at T12 and thalamic Glx (measured at T0). However, none of these survived the correction for multiple comparisons. Thus, this study cannot suggest that toenail metal deposition are indicative of changes in metabolite concentration in the thalamus at any timepoint.

Similarly, in our network plot visualization of the correlations between *cerebellar* metabolites and toenail Mn (Fig. 5*D*), the points are also far apart, again, indicating weaker correlations. No association between cerebellar GABA+ with Mn nor Fe could be found, as determined by the lack of connections in the network plot. We did, however, demonstrate a strong positive correlation between cerebellar GSH and toenail Fe at T12, which survived the correction for multiple comparisons. This finding was also confirmed by the results of the GEE model, which is best at estimating population-averaged effects, rather than individual-specific effects (such as in general mixed models), as suggested in (Hubbard et al., 2010). Since toenail levels reflect metal exposure and deposition into toenail tissue 7–12 months prior to clipping the nail, deposition of Fe measured at T12 occurs at T0-T6, which includes the time when brain GSH levels were measured (T0). Therefore, the significant cerebellar GSH-Fe correlation at T12 may cautiously be interpreted that as Fe deposition into toenails increases, GSH also increases in the cerebellum. Because glutathione has a cyclic pathway, it exists in two forms, reduced (GSH – most abundant) and oxidized (GSSG). (Aquilano et al., 2014) With MRS, we quantify GSH in its reduced form. Therefore, we infer that decreased levels of GSH measured by MRS indicate a down-regulation of GSH and an increase in GSSG (and thereby increased oxidative stress), whereas an increase in GSH may be taken as an upregulation in response to a rise in ROS. Adding this common interpretation of GSH levels measured by MRS, the significant GSH-Fe correlation at T12 may reflect increased ROS caused by exposure at the time of the brain scan.

Our data replicates that toenail metal levels are intercorrelated across different time points, as already reported by Ward et al., (2018). The intercorrelations strongly depend on any changes in exposure that occurred for the specific group of welders at any given time, which will vary from study to study. In our data the strong correlations between toenail Mn at T0 and T3 indicates that exposure was rather stable a year to nine months prior to MRI, while possibly more changes happened at later time points, which show lower correlations. The fact that Mn and Fe toenail levels may correlate is explained by the welding electrodes having a fixed ratio of the two metals. Therefore, a correlation is expected unless there are changes in welding practice or materials in the work environment, which occurs occasionally in the occupational environment (e.g. change of welding station). Lastly, the ICC results further support these findings by quantifying the intrasubject correlations of the measurements, which may indicate strong consistency of exposure amongst welders and thus contribute to their normal range of variation in toenail metal levels.

As mentioned before, it is important to note the limitations of this study. While we began with a sample size of 22, the number of welders who had a good quality MRI/MRS and toenail dataset (n = 17) and the sample size of obtained toenail clippings at each time point after T0 (n = 8–10 strongly limit the generalization of the results. Furthermore, unfortunately, the welders with the highest exposure among the group (in terms of total airborne exposure and clear T1w hyperintensities in the GP) did not continue to supply toenails after their first visit. Another limitation of this study is the lack of a proper control group for the full longitudinal study design. However, the results from annual toenail data obtained from six controls in the parent study with the same methods serve to demonstrate the elevated toenail levels in the study's welder cohort and to compare the variability of toenail sampling over one year.

In conclusion, our results were not able to support a role for toenail

Mn as a biomarker for brain Mn levels or metabolic changes. However, this does not discount toenails as a sensitive and specific biomarker of airborne exposure to Mn in career welders, as suggested by multiple groups (Grashow et al., 2014; Laohaudomchok et al., 2011; Ward et al., 2018), or that toenails are not associated with other exposure metrics. Nonetheless, toenail Fe may be more associated with brain Fe deposition and metabolic changes. Overall, our results may suggest that the uptake of metals into the brain versus toenails is too distinct and complex to allow for toenail metal levels to serve as a proxy of changes in brain metabolism. Lastly, our results suggest that Fe may play a role in Mn neurotoxicity and that other metals involved in Mn homeostasis should also be considered in the study of Mn neurotoxicity.

CRediT authorship contribution statement

Ulrike Dydak: Writing – review & editing, Writing – original draft, Supervision, Resources, Project administration, Investigation, Funding acquisition, Conceptualization. **Ellen M Wells:** Writing – review & editing, Formal analysis. **Jae Hong Park:** Writing – review & editing, Supervision, Resources. **Chang Geun Lee:** Writing – review & editing, Visualization, Investigation, Data curation. **Grace Francis:** Formal analysis. **Gianna Nossa:** Writing – review & editing, Writing – original draft, Visualization, Software, Investigation, Formal analysis, Data curation. **Humberto Monsivais:** Writing – review & editing, Writing – original draft, Visualization, Software, Investigation, Formal analysis, Data curation.

Declaration of Competing Interest

The authors declare the following financial interests/personal relationships which may be considered as potential competing interests: Ulrike Dydak reports a relationship with American Regent Inc that includes: consulting or advisory. If there are other authors, they declare that they have no known competing financial interests or personal relationships that could have appeared to influence the work reported in this paper.

Data availability

Data will be made available on request.

Acknowledgements

We would like to acknowledge Sandy Snyder for her help with recruitment. This work was supported by the International Manganese Institute, National Institute of Health (NIH)/National Institute of Environmental Health Sciences (NIEHS) R01 ES032478 (UD) and F31 ES035299 (HM). This research was also partially supported by the National Institute for Occupational Safety and Health (NIOSH) through the Pilot Research Project Training Program of the University of Cincinnati Education and Research Center Grant (T42 OH008432) and through the Pilot Project Research Training Program of the University of Michigan Education and Research Center Grant (T42 OH008455).

References

Aquilano, K., Baldelli, S., Ciriolo, M.R., 2014. Glutathione: new roles in redox signaling for an old antioxidant. Front. Pharmacol. *5* (196), 1–15. https://doi.org/10.3389/fphar.2014.00196.

Aschner, J.L., Aschner, M., 2005. Nutritional aspects of manganese homeostasis. Mol. Asp. Med *26* (4–5), 353–362. https://doi.org/10.1016/j.mam.2005.07.003.

Ashburner, J., 2007. A fast diffeomorphic image registration algorithm. NeuroImage *38*, 95–113. https://doi.org/10.1016/j.neuroimage.2007.07.007.

Baillieux, H., De Smet, H.J., Paquier, P.F., De Deyn, P.P., Mariën, P., 2008. Cerebellar neurocognition: insights into the bottom of the brain. Clin. Neurol. Neurosurg. *110*, 763–773. https://doi.org/10.1016/j.clineuro.2008.05.013.

Baker, M., Criswell, S., Racette, B., Simpson, C., Sheppard, L., Checkoway, H., Seixas, N., 2015. Neurological outcomes associated with low-level manganese exposure in an inception cohort of asymptomatic welding trainees. Scand. J. Work Environ. Health *41* (1), 94–101. https://doi.org/10.5271/sjweh.3466.

Beaton, A., Mariën, P., 2010. Language, cognition and the cerebellum: grappling with an enigma. CORTEX *46*, 811–820. https://doi.org/10.1016/j.cortex.2010.02.005.

Chan, K.L., Puts, N.A.J., Schär, M., Barker, P.B., Edden, R.A.E., 2016. HERMES: hadamard encoding and reconstruction of MEGA-edited spectroscopy. Magn. Reson. Med. *76* (1), 11. https://doi.org/10.1002/MRM.26233.

Chang, Y., Woo, S.T., Lee, J.J., Song, H.J., Lee, H.J., Yoo, D.S., Kim, S.H., Lee, H., Kwon, Y.J., Ahn, H.J., Ahn, J.H., Park, S.J., Weon, Y.C., Chung, I.S., Jeong, K.S., Kim, Y., 2009. Neurochemical changes in welders revealed by proton magnetic resonance spectroscopy. NeuroToxicology *30* (6), 950–957. https://doi.org/10.1016/J.NEURO.2009.07.008.

Chang, Y., Jin, S.U., Kim, Y., Shin, K.M., Lee, H.J., Kim, S.H., Ahn, J.H., Park, S.J., Jeong, K.S., Weon, Y.C., Lee, H., 2013. Decreased brain volumes in manganese-exposed welders. NeuroToxicology *37*, 182–189. https://doi.org/10.1016/J.NEURO.2013.05.003.

Chen, P., Chakraborty, S., Mukhopadhyay, S., Lee, E., Paoliello, M.M., Bowman, A.B., Aschner, M., 2015. Manganese homeostasis in the nervous system. J. Neurochem *134*, 601–610. https://doi.org/10.1111/jnc.13170.

Cowan, D.M., Zheng, W., Zou, Y., Shi, X., Chen, J., Rosenthal, F.S., Fan, Q., Zheng, W., 2009. Manganese exposure among smelting workers: Relationship between blood manganese-iron ratio and early onset neurobehavioral alterations. Neurotoxicology *30* (6), 1214–1222. https://doi.org/10.1016/j.neuro.2009.02.005.

Criswell, S.R., Perlmutter, J.S., Huang, J.L., Golchin, N., Flores, H.P., Hobson, A., Aschner, M., Erikson, K.M., Checkoway, H., Racette, B.A., Environ, O., Author, M., 2012. Basal ganglia intensity indices and diffusion weighted imaging in manganese-exposed welders NIH Public Access Author Manuscript. Occup. Environ. Med *69* (6), 437–443. https://doi.org/10.1136/oemed-2011-100119.

Criswell, S.R., Nelson, G., Gonzalez-Cuyar, L.F., Huang, J., Shimony, J.S., Checkoway, H., Simpson, C.D., Dills, R., Seixas, N.S., Racette, B.A., 2015. Ex-Vivo Magnetic Resonance Imaging in South African Manganese Mine Workers HHS Public Access. Neurotoxicology *49*, 8–14. https://doi.org/10.1016/j.neuro.2015.04.002.

Criswell, S.R., Searles Nielsen, S., Warden, M.N., Flores, H.P., Lenox-Krug, J., Racette, S., Sheppard, L., Checkoway, H., Racette, B.A., Criswell, M., 2019. MRI Signal Intensity and Parkinsonism in Manganese-Exposed Workers HHS Public Access. J. Occup. Environ. Med *61* (8), 641–645. https://doi.org/10.1097/JOM.0000000000001634.

Dorman, D.C., Struve, M.F., Wong, B.A., 2002. Brain Manganese Concentrations in Rats Following Manganese Tetroxide Inhalation are Unaffected by Dietary Manganese Intake. NeuroToxicology *23* (2), 185–195. https://doi.org/10.1016/S0161-813X(01)00075-4.

Dorman, D.C., Struve, M.F., Wong, B.A., Dye, J.A., Robertson, I.D., 2006. Correlation of Brain Magnetic Resonance Imaging Changes with Pallidal Manganese Concentrations in Rhesus Monkeys Following Subchronic Manganese Inhalation. TOXICOLOGICAL Sci. *91* (1), 219–227. https://doi.org/10.1093/toxsci/kfj209.

Du, G., Lewis, M.M., Styner, M., Shaffer, M.L., Sen, S., Yang, Q.X., Huang, X., 2011. Combined R2* and diffusion tenser imaging changes in the substantia nigra in Parkinson disease. Mov. Disord.: Off. J. Mov. Disord. Soc. *26* (9), 1627. https://doi.org/10.1002/MDS.23643.

Duck Park, J., Hyun Chung, Y., Yong Kim, C., Soo Ha, C., Oh Yang, S., Soo Khang, H., Kyu Yu, I., Kwan Cheong, H., Seong Lee, J., Song, C.-W., Hoon Kwon, I., Hee Han, J., Hyuck Sung, J., Doo Heo, J., Sun Choi, B., Im, R., Jeong, J., Je Yu, I., 2007. Comparison of High MRI T1 Signals with Manganese Concentration in Brains of Cynomolgus Monkeys After 8 Months of Stainless Steel Welding-Fume Exposure. Inhal. Toxicol. *19* (11), 965–971. https://doi.org/10.1080/08958370701516108.

Dydak, U., Criswell, S.R., 2015. Imaging Modalities for Manganese Toxicity. In: Costa, L. G., Aschner, M. (Eds.), Manganese in Health and Disease. Royal Society of Chemistry, pp. 477–501. https://doi.org/10.1039/9781782622383-00477.

Dydak, U., Jiang, Y.M., Long, L.L., Zhu, H., Chen, J., Li, W.M., Edden, R.A.E., Hu, S., Fu, X., Long, Z., Mo, X.A., Meier, D., Harezlak, J., Aschner, M., Murdoch, J.B., Zheng, W., 2011. In Vivo Measurement of Brain GABA Concentrations by Magnetic Resonance Spectroscopy in Smelters Occupationally Exposed to Manganese. Environ. Health Perspect. *119* (2), 219. https://doi.org/10.1289/EHP.1002192.

Edden, R.A.E., Puts, N.A.J., Harris, A.D., Barker, P.B., Evans, C.J., 2014. Gannet: A batch-processing tool for the quantitative analysis of gamma-aminobutyric acid-edited MR spectroscopy spectra. J. Magn. Reson. Imaging *40* (6), 1445–1452. https://doi.org/10.1002/JMRI.24478.

Edmondson, D.A., Ma, R.E., Yeh, C.-L., Ward, E., Snyder, S., Azizi, E., Zauber, S.E., Wells, E.M., Dydak, U., 2019. Reversibility of Neuroimaging Markers Influenced by Lifetime Occupational Manganese Exposure. Toxicol. Sci. *172* (1), 181–190. https://doi.org/10.1093/toxsci/kfz174.

Fitsanakis, V.A., Zhang, N., Avison, M.J., Gore, J.C., Aschner, J.L., Aschner, M., 2006. The use of magnetic resonance imaging (MRI) in the study of manganese neurotoxicity. Neurotoxicology *27*, 798–806. https://doi.org/10.1016/j.neuro.2006.03.001.

Gelman, N., Gorell, J.M., Barker, P.B., Savage, R.M., Spickler, E.M., Windham, J.P., Knight, R.A., 1999. MR Imaging Hum. Brain 3. 0 T: Prelim. Rep. Transverse Relax. Rates Relat. Estim. Iron Content *210* (3), 759–767. https://doi.org/10.1148/RADIOLOGY.210.3.R99FE41759. Https://Doi.Org/10.1148/Radiology.210.3.R99fe41759.

Grashow, R., Zhang, J., Fang, S.C., Weisskopf, M.G., Christiani, D.C., Cavallari, J.M., 2014. Toenail metal concentration as a biomarker of occupational welding fume exposure HHS Public Access. J. Occup. Environ. Hyg. *11* (6), 397–405. https://doi.org/10.1080/15459624.2013.875182.

Griffiths, P.D., Dobson, B.R., Jones, G.R., Clarke, D.T., 1999. Iron in the basal ganglia in Parkinson's diseaseAn in vitro study using extended X-ray absorption fine structure

and cryo-electron microscopy. Brain *122* (4), 667–673. https://doi.org/10.1093/BRAIN/122.4.667.
Grünecker, B., Kaltwasser, S.F., Zappe, A.C., Bedenk, B.T., Bicker, Y., Spoormaker, V.I., Wotjak, C.T., Czisch, M., 2013. Regional specificity of manganese accumulation and clearance in the mouse brain: implications for manganese-enhanced MRI. NMR Biomed. *26* (5), 542–556. https://doi.org/10.1002/NBM.2891.
Guilarte, T.R., Chen, M.K., McGlothan, J.L., Verina, T., Wong, D.F., Zhou, Y., Alexander, M., Rohde, C.A., Syversen, T., Decamp, E., Koser, A.J., Fritz, S., Gonczi, H., Anderson, D.W., Schneider, J.S., 2006. Nigrostriatal dopamine system dysfunction and subtle motor deficits in manganese-exposed non-human primates. Exp. Neurol. *202* (2), 381–390. https://doi.org/10.1016/J.EXPNEUROL.2006.06.015.
Guilarte, T.R., Burton, N.C., Mcglothan, J.L., Verina, T., Zhou, Y., Alexander, M., Pham, L., Griswold, M., Wong, D.F., Syversen, T., Schneider, J.S., 2008. Impairment of nigrostriatal dopamine neurotransmission by manganese is mediated by pre-synaptic mechanism(s): Implications to manganese-induced parkinsonism. NIH Public Access. *J. Neurochem 107* (5), 1236–1247. https://doi.org/10.1111/j.1471-4159.2008.05695.x.
Haacke, E.M., Cheng, N.Y.C., House, M.J., Liu, Q., Neelavalli, J., Ogg, R.J., Khan, A., Ayaz, M., Kirsch, W., Obenaus, A., 2005. Imaging iron stores in the brain using magnetic resonance imaging. Magn. Reson. Imaging *23* (1), 1–25. https://doi.org/10.1016/J.MRI.2004.10.001.
Haber, S.N., Calzavara, R., 2009. The cortico-basal ganglia integrative network: the role of the thalamus. Brain Res. Bull. *78*, 69–74. https://doi.org/10.1016/j.brainresbull.2008.09.013.
Horning, K.J., Caito, S.W., Tipps, K.G., Bowman, A.B., Aschner, M., 2015. Manganese Is Essential for Neuronal Health. Annu. Rev. Nutr. *35* (1), 71–108. https://doi.org/10.1146/ANNUREV-NUTR-071714-034419.
Hubbard, A.E., Ahern, J., Fleischer, N.L., Laan, M., Van Der Lippman, S.A., Jewell, N., Bruckner, T., Satariano, W.A., 2010. To GEE or not to GEE: Comparing population average and mixed models for estimating the associations between neighborhood risk factors and health. Epidemiology *21* (4), 467–474. https://doi.org/10.1097/EDE.0B013E3181CAEB90.
Jankovic, J., 2005. Motor fluctuations and dyskinesias in Parkinson's disease: Clinical manifestations. Mov. Disord. *20* (S11), S11–S16. https://doi.org/10.1002/MDS.20458.
Josephs, K.A., Ahlskog, J.E., Klos, K.J., Kumar, N., Fealey, R.D., Trenerry, M.R., Cowl, C. T., 2005. Neurologic manifestations in welders with pallidal MRI T1 hyperintensity. Neurology *64* (12), 2033–2039. https://doi.org/10.1212/01.WNL.0000167411.93483.A1.
Karyakina, N.A., Shilnikova, N., Farhat, N., Ramoju, S., Cline, B., Momoli, F., Mattison, D., Jensen, N., Terrell, R., Krewski, D., 2022. Biomarkers for occupational manganese exposure. Crit. Rev. Toxicol. *52* (8), 636–663. https://doi.org/10.1080/10408444.2022.2128718.
Kim, E.A., Cheong, H.K., Choi, D.S., Sakong, J., Ryoo, J.W., Park, I., Kang, D.M., 2007. Effect of occupational manganese exposure on the central nervous system of welders: 1H magnetic resonance spectroscopy and MRI findings. Neurotoxicology *28* (2), 276–283. https://doi.org/10.1016/J.NEURO.2006.05.013.
Koo, T.K., Li, M.Y., 2016. A Guideline of Selecting and Reporting Intraclass Correlation Coefficients for Reliability Research. J. Chiropr. Med. *15* (2), 155. https://doi.org/10.1016/J.JCM.2016.02.012.
Koziol, L.F., Budding, D., Andreasen, N., D'arrigo, S., Bulgheroni, S., Imamizu, H., Ito, M., Manto, M., Marvel, C., Parker, K., Pezzulo, G., Ramnani, N., Riva, D., Schmahmann, J., Vandervert, L., Yamazaki, T., 2014. Consensus Paper: The Cerebellum's Role in Movement and Cognition. Cerebellum *13*, 151–177. https://doi.org/10.1007/s12311-013-0511-x.
Laohaudomchok, W., Lin, X., Herrick, R.F., Fang, S.C., Cavallari, J.M., Christiani, D.C., Weisskopf, M.G., 2011. Toenail, Blood and Urine as Biomarkers of Manganese Exposure. J. Occup. Environ. Med *53* (5), 506–510. https://doi.org/10.1097/JOM.0b013e31821854da.
Lee, C.G., Lee, J.H., Specht, A., Liu, S., Dydak, U., Park, J.H., 2023. Comparison of X-Ray Fluorescence (XRF) and Inductively Coupled Plasma-Optical Emission spectrometry (ICP-OES) with ICP-mass spectrometry (ICP-MS) for the Measurement of Toenail Metal Levels. Soc. Toxicol. 62nd Annu. Meet. 32478.
Lee, E.-Y., Flynn, M.R., Du, G., Lewis, M.M., Fry, R., Herring, A.H., Van Buren, E., Van Buren, S., Smeester, L., Kong, L., Yang, Q., Mailman, R.B., Huang, X., 2015. T1 Relaxation Rate (R1) Indicates Nonlinear Mn Accumulation in Brain Tissue of Welders With Low-Level Exposure. TOXICOLOGICAL Sci. *146* (2), 281–289. https://doi.org/10.1093/toxsci/kfv088.
Lee, E.-Y., Flynn, M.R., Du, G., Li, Y., Lewis, M.M., Herring, A.H., Van Buren, E., Van Buren, S., Kong, L., Fry, R.C., Snyder, A.M., Connor, J.R., Yang, Q.X., Mailman, R.B., Huang, X., 2016. Increased R2* in the Caudate Nucleus of Asymptomatic Welders. TOXICOLOGICAL Sci. *150* (2), 369–377. https://doi.org/10.1093/toxsci/kfw003.
Lewis, M.M., Lee, E.Y., Jo, H.J., Du, G., Park, J., Flynn, M.R., Kong, L., Latash, M.L., Huang, X., 2016. Synergy as a new and sensitive marker of basal ganglia dysfunction: A study of asymptomatic welders. NeuroToxicology *56*, 76–85. https://doi.org/10.1016/J.NEURO.2016.06.016.
Lewis, M.M., Flynn, M.R., Lee, E.Y., Van Buren, S., Van Buren, E., Du, G., Fry, R.C., Herring, A.H., Kong, L., Mailman, R.B., Huang, X., 2016. Longitudinal T1 relaxation rate (R1) captures changes in short-term Mn exposure in welders. Neurotoxicology *57*, 39. https://doi.org/10.1016/J.NEURO.2016.08.012.
Liang, K.-Y., Zeger, S.L., 1986. Longitudinal data analysis using generalized linear models. Biometrika *73* (1), 13–22. ⟨https://academic.oup.com/biomet/article/73/1/13/246001⟩.
Liang, X., Saleh, M.G., Xu, S., Mayer, D., Roys, S., Raghavan, P., Badjatia, N., Gullapalli, R.P., Zhuo, J., 2024. Simultaneous Measurement of GABA, Glutathione, and Glutamate–Glutamine in the Thalamus using Edited MR Spectroscopy: Feasibility and Applications in Traumatic Brain Injury. J. Magn. Reson. Imaging. https://doi.org/10.1002/JMRI.29299.
Lin, M., Colon-Perez, L.M., Sambo, D.O., Miller, D.R., Lebowitz, J.J., Jimenez-Rondan, F., Cousins, R.J., Horenstein, N., Aydemir, T.B., Febo, M., Khoshbouei, H., 2020. Neurobiology of Disease Mechanism of Manganese Dysregulation of Dopamine Neuronal Activity. J. Neurosci. *40* (30), 5871–5891. https://doi.org/10.1523/JNEUROSCI.2830-19.2020.
Lin, Q., Shahid, S., Hone-Blanchet, A., Huang, S., Wu, J., Bisht, A., Loring, D., Goldstein, F., Levey, A., Crosson, B., Lah, J., Qiu, D., 2023. Magnetic resonance evidence of increased iron content in subcortical brain regions in asymptomatic Alzheimer's disease. Hum. Brain Mapp. *44* (8), 3072–3083. https://doi.org/10.1002/HBM.26263.
Lipe, G.W., Duhart, H., Newport, G.D., Slikker, W., Ali, S.F., 1999. Effect of manganese on the concentration of amino acids in different regions of the rat brain. J. Environ. Sci. Health Part. B, Pestic., Food Contam., Agric. Wastes *34* (1), 119–132. https://doi.org/10.1080/03601239909373187.
Long, Z., Jiang, Y.M., Li, X.R., Fadel, W., Xu, J., Yeh, C.L., Long, L.L., Luo, H.L., Harezlak, J., Murdoch, J.B., Zheng, W., Dydak, U., 2014a. Vulnerability of Welders to Manganese Exposure – A Neuroimaging Study. Neurotoxicology *0*, 285. https://doi.org/10.1016/J.NEURO.2014.03.007.
Long, Z., Li, X.R., Xu, J., Edden, R.A.E., Qin, W.P., Long, L.L., Murdoch, J.B., Zheng, W., Jiang, Y.M., Dydak, U., 2014b. Thalamic GABA Predicts Fine Motor Performance in Manganese-Exposed Smelter Workers. PLOS ONE *9* (2), e88220. https://doi.org/10.1371/JOURNAL.PONE.0088220.
Lorio, S., Lutti, A., Kherif, F., Ruef, A., Dukart, J., Chowdhury, R., Frackowiak, R.S., Ashburner, J., Helms, G., Weiskopf, N., Draganski, B., 2014. Disentangling in vivo the effects of iron content and atrophy on the ageing human brain. NeuroImage *103*, 280–289. https://doi.org/10.1016/j.neuroimage.2014.09.044.
Lucchini, R.G., Guazzetti, S., Zoni, S., Donna, F., Peter, S., Zacco, A., Salmistraro, M., Bontempi, E., Zimmerman, N.J., Smith, D.R., 2012. Tremor, olfactory and motor changes in Italian adolescents exposed to historical ferro-manganese emission. Neurotoxicology *33*, 687–696. https://doi.org/10.1016/j.neuro.2012.01.005.
Ma, R.E., Ward, E.J., Yeh, C.L., Snyder, S., Long, Z., Gokalp Yavuz, F., Zauber, S.E., Dydak, U., 2018. Thalamic GABA levels and Occupational Manganese Neurotoxicity: Association with Exposure Levels and Brain MRI. Neurotoxicology *64*, 30. https://doi.org/10.1016/J.NEURO.2017.08.013.
McCarthy, P. (2023). *FSLeyes* (1.10.0). Zenodo. ⟨https://doi.org/10.5281/ZENODO.10122614⟩.
Monsivais, H., Yeh, C.-L., Edmondson, A., Harold, R., Snyder, S., Wells, E.M., Schmidt-Wilcke, T., Foti, D., Zauber, S.E., Dydak, U., 2024. Whole-brain mapping of increased manganese levels in welders and its association with exposure and motor function. NeuroImage *288*, 120523. https://doi.org/10.1016/J.NEUROIMAGE.2024.120523.
Murdoch, B.E., 2010. Special issue: Review The cerebellum and language: Historical perspective and review. CORTEX *46*, 858–868. https://doi.org/10.1016/j.cortex.2009.07.018.
Nicola, S.M., James, D., Malenka, R.C., 2000. DOPAMINERGIC MODULATION OF NEURONAL EXCITABILITY IN THE STRIATUM AND NUCLEUS ACCUMBENS. Annu. Rev. Neurosci. *23*, 185–215. ⟨www.annualreviews.org⟩.
O'Neal, S.L., Zheng, W., 2015. Manganese Toxicity Upon Overexposure: a Decade in Review. Curr. Environ. Health Rep. *2* (3), 315. https://doi.org/10.1007/S40572-015-0056-X.
Péran, P., Cherubini, A., Assogna, F., Piras, F., Quattrocchi, C., Peppe, A., Celsis, P., Rascol, O., Démonet, J.F., Stefani, A., Pierantozzi, M., Pontieri, F.E., Caltagirone, C., Spalletta, G., Sabatini, U., 2010. Magnetic resonance imaging markers of Parkinson's disease nigrostriatal signature. Brain *133* (11), 3423–3433. https://doi.org/10.1093/BRAIN/AWQ212.
Raab, A., Feldmann, J., 2005. Arsenic speciation in hair extracts. Anal. Bioanal. Chem. *381* (2), 332–338. ⟨https://doi.org/10.1007/S00216-004-2796-6/FIGURES/3⟩.
Rorden, C., Brett, M., 2000. Stereotaxic display of brain lesions. Behav. Neurol. *12*, 191–200. ⟨www.fil.ion.ucl.ac.uk/spm/⟩.
Rossi, M.E., Ruottinen, H., Saunamäki, T., Elovaara, I., Dastidar, P., 2014. Imaging Brain Iron and Diffusion Patterns. A Follow-up Study of Parkinson's Disease in the Initial Stages. Acad. Radiol. *21* (1), 64–71. https://doi.org/10.1016/j.acra.2013.09.018.
Schmahmann, J.D., Sherman, J.C., 1998. The cerebellar cognitive affective syndrome. Brain *121*, 561–579.
Slotnick, M.J., Nriagu, J.O., 2006. Validity of human nails as a biomarker of arsenic and selenium exposure: A review. Environ. Res. *102* (1), 125–139. https://doi.org/10.1016/J.ENVRES.2005.12.001.
Stoodley, C.J., Schmahmann, J.D., 2010. Evidence for topographic organization in the cerebellum of motor control versus cognitive and affective processing. CORTEX *46*, 831–844. https://doi.org/10.1016/j.cortex.2009.11.008.
Tabelow, K., Balteau, E., Ashburner, J., Callaghan, M.F., Draganski, B., Helms, G., Kherif, F., Leutritz, T., Lutti, A., Phillips, C., Reimer, E., Ruthotto, L., Seif, M., Weiskopf, N., Ziegler, G., Mohammadi, S., 2019. hMRI – A toolbox for quantitative MRI in neuroscience and clinical research. Neuroimage *194*, 191. https://doi.org/10.1016/J.NEUROIMAGE.2019.01.029.
Takeda, A., Sawashita, J., Okada, S., 1995. Biological half-lives of zinc and manganese in rat brain. Brain Res. *695* (1), 53–58. https://doi.org/10.1016/0006-8993(95)00916-E.
Tjillve, H., Henriksson, J., Tallkvist, J., Larsson, B.S., Lindquist, N.G., 1996. Uptake of Manganese and Cadmium from the Nasal Mucosa into the Central Nervous System via Olfactory Pathways in Rats. Pharmacol. Toxicol. *79*, 347–356. https://doi.org/10.1111/j.1600-0773.1996.tb00021.x.
Tuschl, K., Mills, P.B., Clayton, P.T., 2013. Manganese and the Brain. Int. Rev. Neurobiol. *110*, 277–312. https://doi.org/10.1016/B978-0-12-410502-7.00013-2.

Ulla, M., Bonny, J.M., Ouchchane, L., Rieu, I., Claise, B., Durif, F., 2013. Is R2* a New MRI Biomarker for the Progression of Parkinson's Disease? A Longitudinal Follow-Up. PLoS ONE *8* (3). https://doi.org/10.1371/JOURNAL.PONE.0057904.

Verhoeven, W.M., Egger, J.I., Kuijpers, H.J., 2011. Manganese and acute paranoid psychosis: A case report. J. Med. Case Rep. *5* (1), 1–4. ⟨https://doi.org/10.1186/1752-1947-5-146/FIGURES/1⟩.

Verina, T., Schneider, J.S., Guilarte, T.R., 2013. Manganese exposure induces-synuclein aggregation in the frontal cortex of non-human primates. Toxicol. Lett. *217*, 177–183. https://doi.org/10.1016/j.toxlet.2012.12.006.

Ward, E.J., Edmondson, D.A., Nour, M.M., Snyder, S., Rosenthal, F.S., Dydak, U., 2018. Toenail Manganese: A Sensitive and Specific Biomarker of Exposure to Manganese in Career Welders. Ann. Work Expo. Health *62* (1), 101. https://doi.org/10.1093/ANNWEH/WXX091.

Yeh, Chien-Lin, Ward, Eric, Snyder, Sandy, Rosenthal Frank, Dydak, U., 2015. Manganese Accumulation in Brain and Toenails reflect Different Time Periods of Exposure. Proc. Int. Soc. Magn. Reson. Med. *23* (2006), 2831.

Zhang, N., Fitsanakis, V.A., Erikson, K.M., Aschner, M., Avison, M.J., Gore, J.C., 2009. A model for the analysis of competitive relaxation effects of manganese and iron in vivo. NMR Biomed. *22* (4), 391. https://doi.org/10.1002/NBM.1348.